Supplementary Materials for

Oxygen Evolution Catalysis by Manganese Oxides Resilient to Voltage Fluctuations

Authors: Ailong Li[1*], Hideshi Ooka[1], Shuang Kong[1], Kiyohiro Adachi[2], Sun Hee Kim[3,4], Daisuke Hashizume[2], Ryuhei Nakamura[1,5*]

Affiliations:

[1]Biofunctional Catalyst Research Team, RIKEN Center for Sustainable Resource Science (CSRS), 2-1 Hirosawa, Wako, Saitama, 351-0198, Japan

[2]Materials Characterization Support Team, RIKEN Center for Emergent Matter Science (CEMS), 2-1 Hirosawa, Wako, Saitama, 351-0198, Japan

[3]Metropolitan Seoul Center, Korea Basic Science Institute, Seoul, 03759, Republic of Korea

[4]Department of Chemistry, Chung-Ang University, Seoul, 06974, Republic of Korea

[5]Earth-Life Science Institute (ELSI), Institute of Science Tokyo, 2-12-1-I7E Ookayama, Meguro-ku, Tokyo, 152-8550, Japan

*Corresponding author: ailong.li@riken.jp, ryuhei.nakamura@riken.jp

Materials and Methods

Electrode Fabrication

MnO_2 on an FTO substrate (7 Ω/sq surface resistivity, NPV-CFT2-7, AsOne, Japan) was synthesized by a thermal decomposition method. Briefly, 0.5 mL of 2 M $Mn(NO_3)_2$ was dropped onto a clean FTO-coated glass and then calcined on a hotplate at 250 °C in air for 6 h. The resulting electrode was rinsed with Milli-Q ultra-pure water (18.2 MΩ cm at 25 °C, Merck Millipore), sonicated for 10 s, and then dried at 40 °C before measurements. A quartz crystal microbalance **(**QCM) electrode was prepared by a spray deposition method. Briefly, an $Mn(NO_3)_2$ solution (4 M) was sprayed onto clean QCM quartz crystals (Platinum-coated, 10 MHz, Hokuto Denko Corp.), which were then heated at 250 °C for 12 h. MnO_2 was only deposited within the platinum coated area (defined using a mask) of the QCM quartz crystal.

Kinetics analysis of the Guyard reaction

In-situ UV-Vis absorption spectra were obtained in diffuse transmission mode using a UV-Vis spectrometer (UV-2550, Shimadzu) equipped with a multipurpose large-sample compartment with a built-in integrating sphere (MPC-2200, Shimadzu). The kinetics of the Guyard reaction[1-3] ($Mn^{7+} + 4\ Mn^{2+} \rightarrow 5\ Mn^{3+}$) was studied spectrophotometrically by recording the time course of absorbance at 545 nm. For the *in-situ* acquisition of spectra, the reactor was placed in front of the integrating sphere to collect the diffuse transmission light.

EPR measurement in parallel and perpendicular modes

EPR measurements were performed using a Bruker EMX/Plus spectrometer equipped with a parallel and perpendicular dual-mode cavity (ER 4116DM)[4]. The temperature was controlled using a liquid He quartz cryostat (Oxford Instruments ESR900) equipped with a temperature and gas flow controller (Oxford Instruments ITC503). The experimental conditions were as follows: microwave frequency: 9.64 GHz (perpendicular mode) and 9.38 GHz (parallel mode); modulation amplitude: 10 G; modulation frequency: 100 kHz; microwave power: 0.03 mW (perpendicular mode) and 5.2 mW (parallel mode), temperature: 4 K; and sweep time: 232 s (perpendicular mode) and 100 s (parallel mode). EPR spectra were collected for different Mn oxidation states using the following modes: Mn^{7+}, [Ar] $3d^0$, S = 0 (EPR silent in both modes);

Mn^{2+} [Ar]$3d^5$, S= 5/2 (EPR active in perpendicular mode); Mn^{3+}, [Ar]$3d^4$, S= 2 (EPR active in parallel mode).

X-ray absorption for oxidation state measurement

X-ray absorption spectra of the Mn K edge were recorded at the BL14B2 beamline of SPring-8. The analysis was performed on the Demeter software platform[5]. The threshold energy (E_0) was determined at the point where the corresponding normalized absorption was equal to 0.5 in a XANES spectrum[6]. The average valence state of Mn was calculated from the linear regression line obtained from standard samples, such as $MnSO_4$, Mn_2O_3, and MnO_2.

***In-situ* resonance Raman measurement**

Resonance Raman spectra were collected on a Raman microscopy system (Senterra, Bruker) using an excitation wavelength of 532 nm. The excitation light was focused on the sample using a microscope objective (Olympus LMPlanFL N 50X/0.5 BD long-focal length objective, 10.6 mm working distance) at a power of 0.5 mW to avoid damage induced by laser radiation. For the measurements, the laser was irradiated through an optical window and the electrolyte onto the working electrode surface.

Electrochemical measurements under fluctuation voltages

Current versus potential curves were obtained with a commercial potentiostat (HZ-5000, Hokuto Denko) at room temperature (25 ± 2 °C). MnO_2 loaded on an FTO substrate (geometric surface area of 1 cm^2), was used as the working electrode and a Pt wire (99.98%, Nilaco) served as the counter electrode. The two electrodes were separated by a proton exchange membrane (Nafion 117, Sigma-Aldrich), which effectively assists in transporting proton ions selectively from the anode to the cathode compartment. The anode chamber was equipped with two optical windows for *in-situ* UV-Vis measurements and time-lapse recording. A sulfuric acid solution (pH 2, with 1.0 M K_2SO_4 as the supporting electrolyte) was used as a base electrolyte, and 1.0 M phosphate (pH 2, prepared using NaH_2PO_4 and H_3PO_4) was added to induce the Guyard reaction.

Cyclic voltammetry

Cyclic voltammetry measurements were conducted in a three-electrode cell. Ag/AgCl/KCl (saturated) was used as a reference electrode. Prior to every electrochemical experiment, the solution resistance was measured and *i*R compensation was then performed manually. Electrode potentials after *i*R compensation were rescaled to the reversible hydrogen electrode (RHE).

QCM measurements

A setup assembled with an HQ-601DK mass sensor (Hokuto Denko) was used for QCM measurements[7]. The frequency changes (Δf) during OER were recorded. Mass changes (Δm) were calculated from Δf according to the Sauerbrey equation:

$$\Delta f = -\frac{2f_0^2 \Delta m}{A_{plezo}(\mu_q \cdot \rho_q)^{1/2}}$$

where f_0 denotes the initial quartz crystal frequency (10 MHz), A_{plezo} is the area of the piezoelectrically active crystal (0.07 cm^{-2}), μ_q is the shear modulus of quartz (2.947 $\times$ 1011 dyn cm^{-2}), and ρ_q is the density of quartz (2.648 g cm^{-3}). The mass sensitivity of the QCM was $\Delta m/\Delta f$ = 0.31 ng Hz^{-1}.

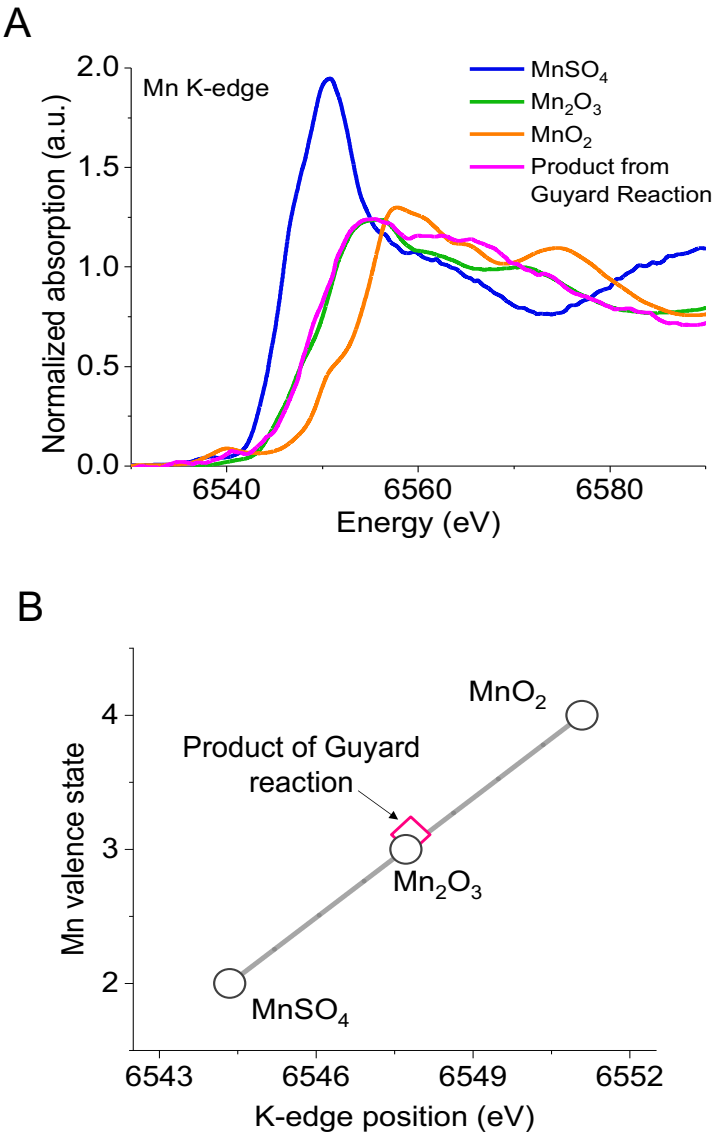

Fig. S1. Normalized Mn K-edge XANES spectra to determine the valence state of manganese. (A) Comparison of the XANES data for the product from the Guyard reaction and reference samples with known oxidation states: Mn^{2+} ($MnSO_4$), Mn^{3+}(Mn_2O_3) and Mn^{4+} (MnO_2). (B) The valence state of the product from the Guyard reaction was estimated to be 3.0 from the linear fitting of the Mn valence and K-edge position, which was defined as the energy where the normalized absorption is 0.5.

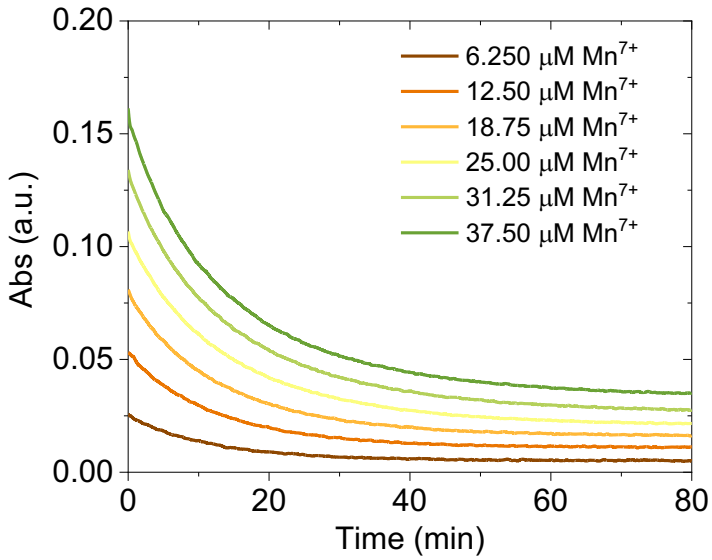

Fig. S2. Measurement of the Guyard reaction kinetics by UV-Vis spectroscopy for Mn^{7+}. Various concentrations of Mn^{7+} (6.25, 12.50, 18.75, 25.00, 31.25, and 37.50 μM) reacted with Mn^{2+} (300 μM) in 1.0 M of phosphate ions at pH 2 and room temperature. The time course of absorbance at 545 nm was plotted to show the reaction kinetics. The reaction was determined to be first order with respect to Mn^{7+}.

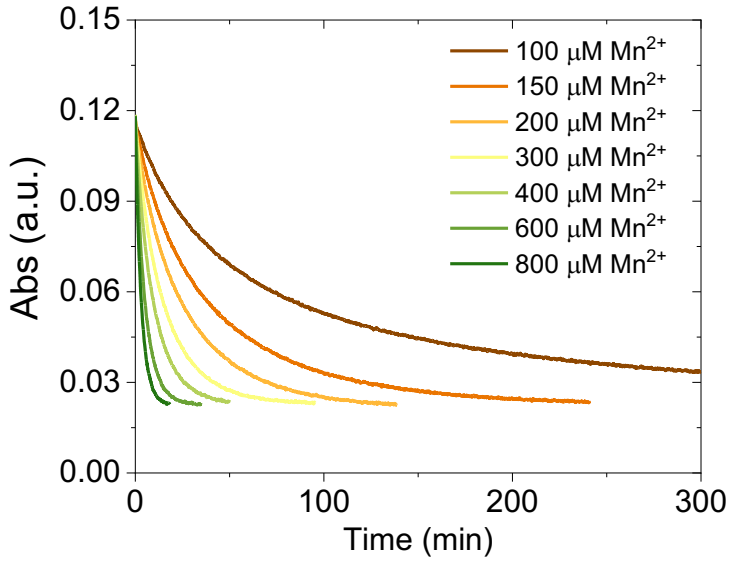

Fig. S3. Measurement of the Guyard reaction kinetics by UV-Vis spectroscopy for Mn^{2+}. Various concentrations of Mn^{2+} (100, 150, 200, 300, 400, 600, and 800 μM) reacted with Mn^{7+} (25 μM) in 1.0 M of phosphate ions at pH 2 and room temperature. The time course of absorbance at 545 nm was plotted to show the reaction kinetics. The reaction was determined to be pseudo-first-order (~1.3) with respect to Mn^{2+}.

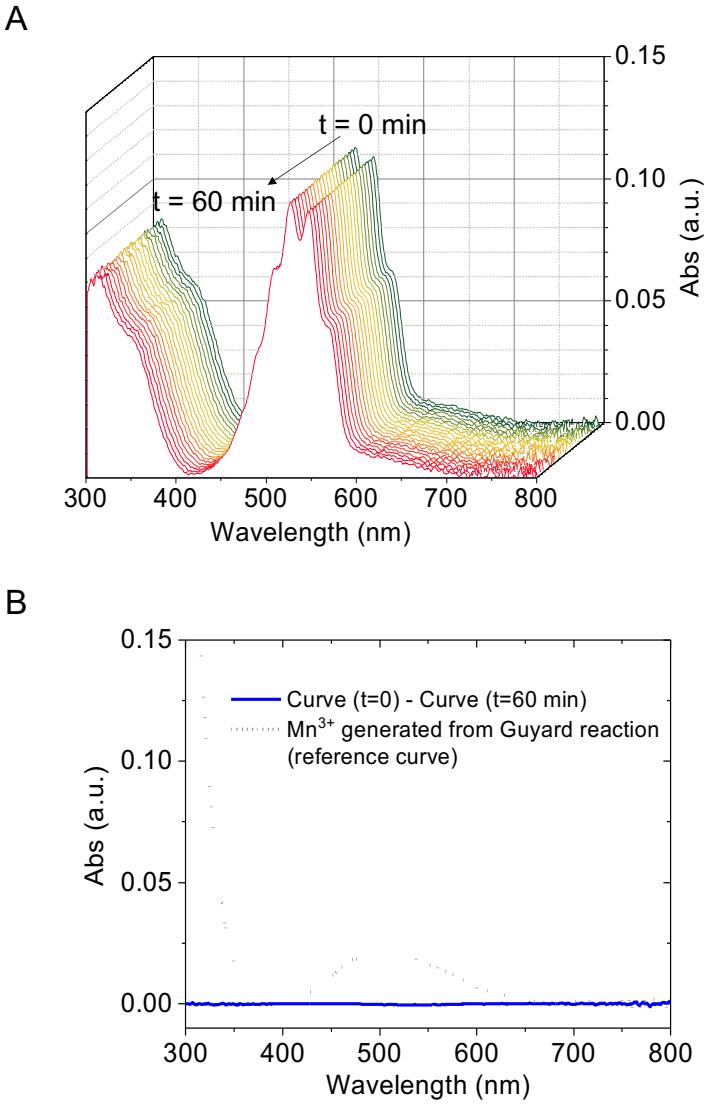

Fig. S4. Measurement of the Guyard reaction kinetics without phosphate ions. (A) UV-Vis spectra of the electrolyte during 1 h of reaction between Mn^{2+} (100 μM) and Mn^{7+} (25 μM) in pH 2 conditions without adding phosphate ions. The base electrolyte was prepared with H_2SO_4 and 1M K_2SO_4. (B) No spectroscopic signatures of Mn^{3+} were observed when the reaction was conducted in sulfuric acid without phosphate ions for 1 h.

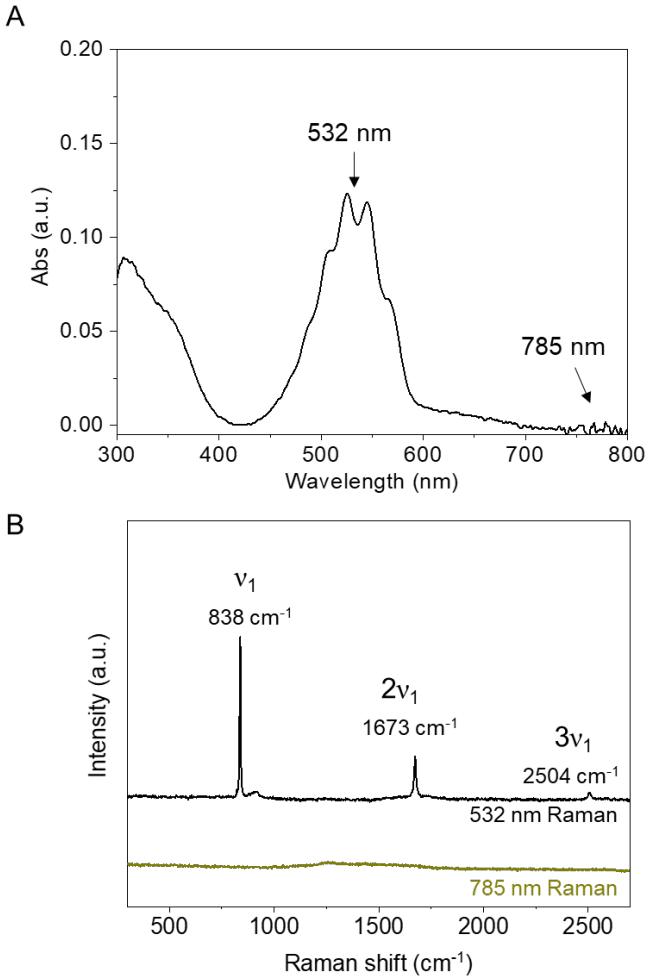

Fig. S5. Resonance Raman spectroscopy for Mn^{7+} measurement. (A) Resonance Raman spectra were collected using an excitation wavelength of 532 nm, which is within the wavelength range where Mn^{7+} shows maximum electronic transition. An excitation wavelength of 785 nm was used for comparison. (B) Raman spectra for Mn^{7+} using excitation wavelengths of 532 and 785 nm. The $\nu_1(A_1)$, $2\nu_1(A_1)$ and $3\nu_1(A_1)$ modes of MnO_4^- ion with T_d symmetry were observed using a resonance excitation wavelength of 532 nm, but these modes were not detected at an excitation wavelength of 785 nm.

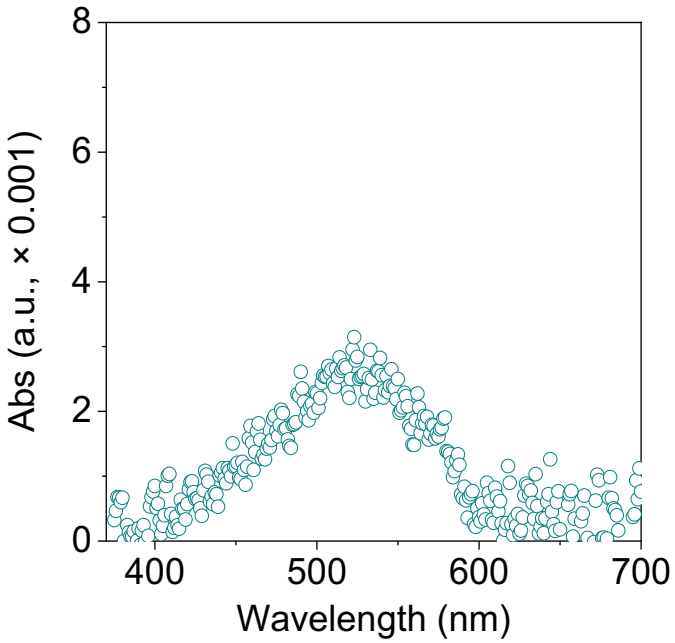

Fig. S6. UV-Vis spectrum of the electrolyte after Raman measurement. The electrolyte was analyzed by UV-Vis spectroscopy after completion of the Raman experiment presented in Fig. 5A.

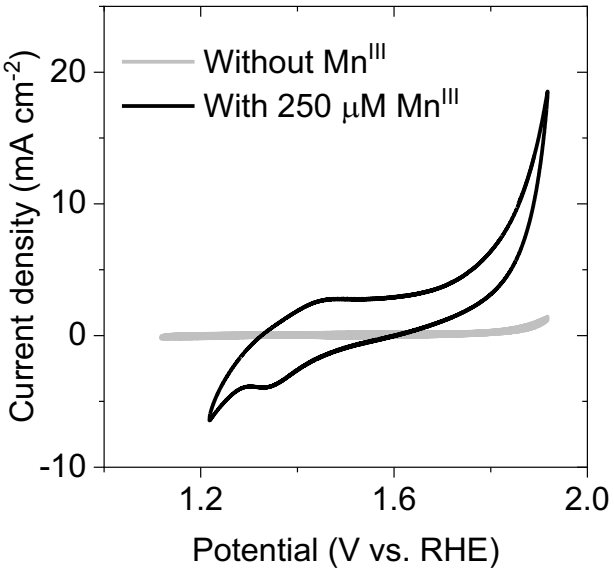

Fig. S7. Cyclic voltametric measurement of Mn^{III}. Cyclic voltametric curves obtained in the presence (black curve) and absence of Mn^{3+} (gray curve). The potentials are relative to reversible hydrogen electrode (RHE).

References:

1 Guyard, A. Of the direct determination of manganese, antimony and uranium by the volumetric method and of several compounds of these metals. *Bull. Soc. Chim. Fr.* **1**, 89-95 (1864).

2 Mrákavová, M. & Treindl, Ł. Kinetics of guyard's reaction with regard to permanganate chemical oscillators. *Collect. Czech. Chem. Commun.* **55**, 2898-2903 (1990).

3 Kovács, K. A., Gróf, P., Burai, L. & Riedel, M. Revising the mechanism of the permanganate/oxalate reaction. *J. Phys. Chem. A* **108**, 11026-11031 (2004).

4 Jin, K. *et al.* Mechanistic investigation of water oxidation catalyzed by uniform, assembled mno nanoparticles. *J. Am. Chem. Soc.* **139**, 2277-2285 (2017).

5 Ravel, B. & Newville, M. ATHENA, ARTEMIS, HEPHAESTUS: data analysis for X-ray absorption spectroscopy using IFEFFIT. *J. Synchrotron Radiat.* **12**, 537-541 (2005).

6 Kong, S. *et al.* Acid-stable manganese oxides for proton exchange membrane water electrolysis. *Nat. Catal.* **7**, 252-261 (2024).

7 Deakin, M. R. & Buttry, D. A. Electrochemical applications of the quartz crystal microbalance. *Anal. Chem.* **61**, 1147A-1154A (1989).